Available online at www.sciencedirect.com
SCIENCE DIRECT®
Electrochimica Acta 50 (2005) 3101–3110
ELECTROCHIMICA Acta
www.elsevier.com/locate/electacta

Self-assembled organic monolayers on gold nanoparticles: A study by sum-frequency generation combined with UV–vis spectroscopy

C. Humbert [a,c,*], B. Busson [a], J.-P. Abid [b], C. Six [a], H.H. Girault [b], A. Tadjeddine [a]

[a] *LURE, CNRS-UMR 130, Centre Universitaire Paris-Sud, Bât. 209D, B.P. 34, 91898 Orsay Cedex, France*
[b] *Ecole Polytechnique Fédérale de Lausanne, Laboratoire d'Electrochimie Physique et Analytique, CH-1015 Lausanne, Switzerland*
[c] *Laboratoire de Spectroscopie Moléculaire de Surface, University of Namur, 61 Rue de Bruxelles, B-5000 Namur, Belgium*

Received 22 July 2004; received in revised form 20 September 2004; accepted 15 October 2004
Available online 2 April 2005

Abstract

We use sum-frequency generation spectroscopy (SFG) in the infrared 2800–3000 cm^{-1} spectral range and UV–vis spectroscopy (transmission) in the 450–650 nm spectral range in order to characterize vibrational and electronic properties of various interfaces composed of organic monolayers adsorbed on gold nanoparticles (AuNPs) with 19 nm average diameter. SFG signal is observed for AuNPs films deposited on glass substrates using the following silane intermediates: 3-(aminopropyl) triethoxysilane and 3-(mercaptopropyl) trimethoxysilane. The density of AuNPs and their aggregates are measured with a scanning electron microscope. For the samples showing a strong well-defined surface plasmon resonance (SPR), we also observe an enhancement of their non-linear optical properties. Furthermore, the SFG measurements show that 1-dodecanethiol films are rather well ordered on specific AuNPs substrates. In this way, the presence of the SFG signal, which comes from both the bulk electronic s–d interband transition and the vibrational states of the adsorbed molecules, depends on a SPR process. This phenomenon is evidenced on the AuNPs by the incident visible beam located at 532 nm, i.e. near the SPR energy maximum of these interfaces. These results open the door to experiments involving macromolecular and biological materials networks deposited on ultrathin metal electrodes in a controlled electrochemical environment.
© 2005 Elsevier Ltd. All rights reserved.

Keywords: Gold nanoparticles; Organic monolayer; Plasmon; Sum-frequency generation; SEM

1. Introduction

Recent developments in electrochemistry have put interest on ultrathin electrodes made of nanoparticles. One of the most extensively and intensively studied system is gold nanoparticles (AuNPs), with various diameters ranging from 5 to 20 nm, showing structural stability under various applied voltage conditions in DC-voltammetry experiment or environment. The fundamentals of AuNPs (synthesis and assembly, physical and chemical properties, biological interest, catalysis and experimental investigation techniques) are well detailed in a recent review article and in the numerous references therein [1]. Our purpose is to apply some recent methods of non-linear optics in order to probe vibrational properties of ordered self-assembled molecular films on these particular metallic electrodes. Until now, research works in non-linear optics such as coherent second harmonic generation (SHG) [2] and incoherent Hyper Rayleigh Scattering (HRS) [3] techniques were limited to the study of AuNPs electronic properties. In vibrational sum-frequency generation (SFG) spectroscopy, one successful attempt of characterization was performed on a cationic surfactant deposited on anionic stabilized AuNPs forming a monolayer on a silicon wafer [4]. Other major works with SFG on nanoparticles are based on catalysis experiments such as in the case of CO molecules adsorbed on Pd or Pt nanoparticles at controlled pressure and temperature [5–7]. In this paper, we characterize by SFG, at ambient conditions, thiolate self-assembled monolayers (SAMs) on AuNPs films. These

* Corresponding author. Tel.: +32 81 724712; fax: +32 81 724718.
E-mail address: christophe.humbert@fundp.ac.be (C. Humbert).

0013-4686/$ – see front matter © 2005 Elsevier Ltd. All rights reserved.
doi:10.1016/j.electacta.2004.10.084

films are deposited on microscope glass substrates by two specific simple appropriate silanisation steps explained hereafter. SFG combined with UV–vis spectroscopy confirms that AuNPs free electrons play a major role in the existence of the SFG process. This is the first step leading to the electrochemical investigation of their interfacial properties with this surface sensitive spectroscopic tool.

2. Samples preparation

2.1. Preparation of the glass substrates

Prior to the silanisation step, the glass substrates were sonicated in a methanolic solution for 20 min and then cleaned in a piranha bath (mixture of 1:4 ratio of H_2O_2 (30%, Fluka) and H_2SO_4 (95–98%, Fluka)). The substrates were rinsed abundantly with absolute ethanol (99.8%, Pancrea) and ultrapure water (conductivity: 0.8 μS cm). After that, the procedure of silanisation was performed using three different methods.

2.1.1. Method 1 (samples A)

The substrates were immersed in a solution of 10% (volume) 3-(aminopropyl) triethoxysilane (95%, Aldrich) in absolute ethanol for 2 h. The samples were carefully washed with absolute ethanol and ultrapure water. The deposition of nanoparticles was performed by immersion of the glass substrates in an aqueous colloidal solution [8] (2.5×10^{-4} M of gold salt) of gold nanoparticles (19 ± 0.21 nm) during 6 h. Finally, the samples were rinsed with ultrapure water. Sample A1 underwent no further treatment. The final step consisted of the immersion of the substrates in a solution of 4.2 mM of dodecanethiol (sample A2) in absolute ethanol for a period of 24 h.

2.1.2. Method 2 (samples B)

The substrates were immersed in a solution of 10% (volume) 3-(mercaptopropyl) trimethoxysilane in absolute ethanol for 2 h. The samples were carefully washed with absolute ethanol and ultrapure water, then immersed in an aqueous colloidal solution (2.5×10^{-4} M of gold salt) of gold nanoparticles (19 ± 0.21 nm) during 6 h. Finally, the samples were rinsed with ultrapure water. The final step consisted of the immersion of the substrates in a solution of 4.2 mM of either dodecanethiol (sample B1) or 2-aminoethanethiol (sample B2) in absolute ethanol for a period of 24 h.

2.1.3. Method 3 (samples C)

As previously described, glass microscope slides were used. The former treatment consisted on soaking the substrates for 30 min in an aqueous solution of NaOH (3 M). The samples were abundantly washed with absolute ethanol and ultrapure water. The second step was the immersion into a 10% solution of 3-(mercaptopropyl) trimethoxysilane in absolute ethanol during 6 h. The substrates were again rinsed with absolute ethanol and ultrapure water. After that, the glass slides were immersed in an aqueous colloidal solution (2.5×10^{-4} M of gold salt) of gold nanoparticles (19 ± 0.21 nm) for a period of 24 h. The samples were rinsed with ultrapure water. The final step was the immersion in a solution of absolute ethanol containing 4.2 mM of either dodecanethiol (sample C1) or 2-aminoethanethiol (sample C2) for 24 h.

3. Spectroscopy and microscopy tools

The UV–vis transmission measurements are carried out with a pulsed Xenon lamp (spectral range: 190–1100 nm, spectral resolution: 1.5 nm) of a Cary 50 Scan (Varian) spectrophotometer. Prior to the measurements, the baseline is set for a clean glass substrate. The SFG measurements are carried out with a tuneable optical parametric oscillator (OPO) built around an $AgGaS_2$ crystal, giving access to the 2000–4000 cm^{-1} infrared spectral range. One part of the amplified energy of a picosecond laser system based on a passive/active mode-locked flash-pumped Nd:YAG laser source [9] is used to pump the OPO. The 15 ps pulses are delivered in a 1 μs train. The OPO bandwidth is 3 cm^{-1} in the 3 μm region with 10 μJ pulse energy. The other part of the YAG beam is frequency-doubled in a BBO crystal to obtain a 532 nm visible radiation with 5 μJ pulse energy. The infrared and visible beams are then mixed at the probed point of the interface with angles of incidence of 65° and 55°, respectively. The beams are p-polarized and the SFG signal is normalized to the one generated by a ZnS reference crystal in order to compensate for laser fluctuations or atmospheric absorption. Transmission electron microscope (TEM) measurements are performed with a Philips CM20 microscope, accelerating voltage 200 kV, LaB6 source, point resolution 2.8 Å, maximum tilt capacity ±45°, absolute minimum probe size ∼2 nm, minimum useful probe size for EDS ∼20 nm in order to deduce the size distribution of the AuNPs in solution. Scanning electron microscope (SEM) measurements are carried out on the samples with a Philips XL 30 FEG high resolution/low accelerating voltage SEM, 1–30 kV field emission SEM, nominal resolution <2 nm at high kV, <8 nm at 1 kV.

4. Spectroscopy and microscopy results

4.1. UV–vis measurements

UV–vis measurements are performed on the samples in the 450–650 nm spectral range, i.e. where the plasmon resonance is expected for 19 nm average diameter AuNPs. The dominant 19 nm average size distribution of the AuNPs is confirmed by TEM measurements (Fig. 1).

For AuNPs attached on glass substrates with 3-(aminopropyl) triethoxysilane (Fig. 2), the clean AuNPs interface (sample A1) and the 1-dodecanethiol/AuNPs

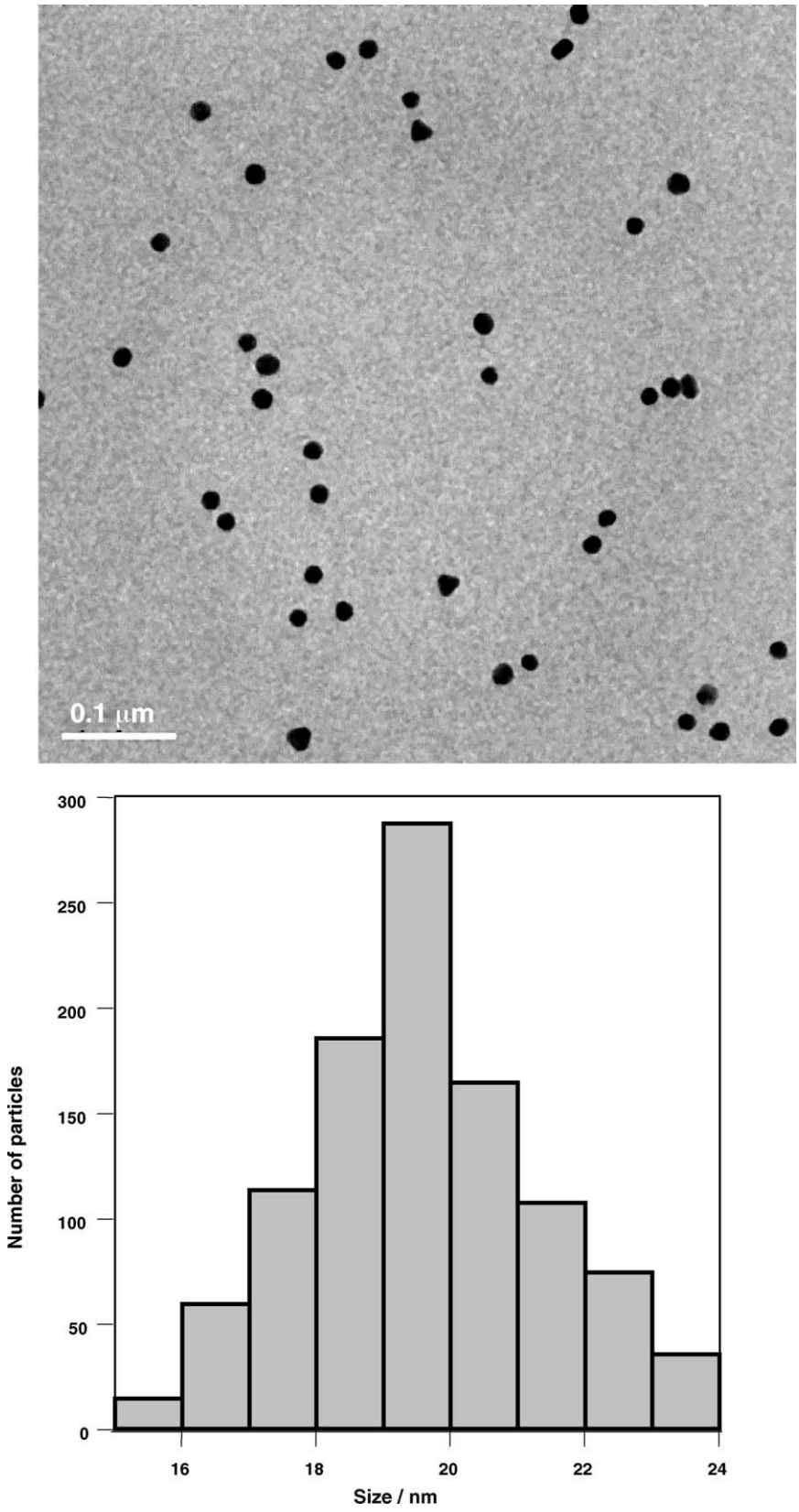

Fig. 1. TEM picture and size distribution of the AuNPs contained in an aqueous colloidal solution. The AuNPs average diameter is 19 nm.

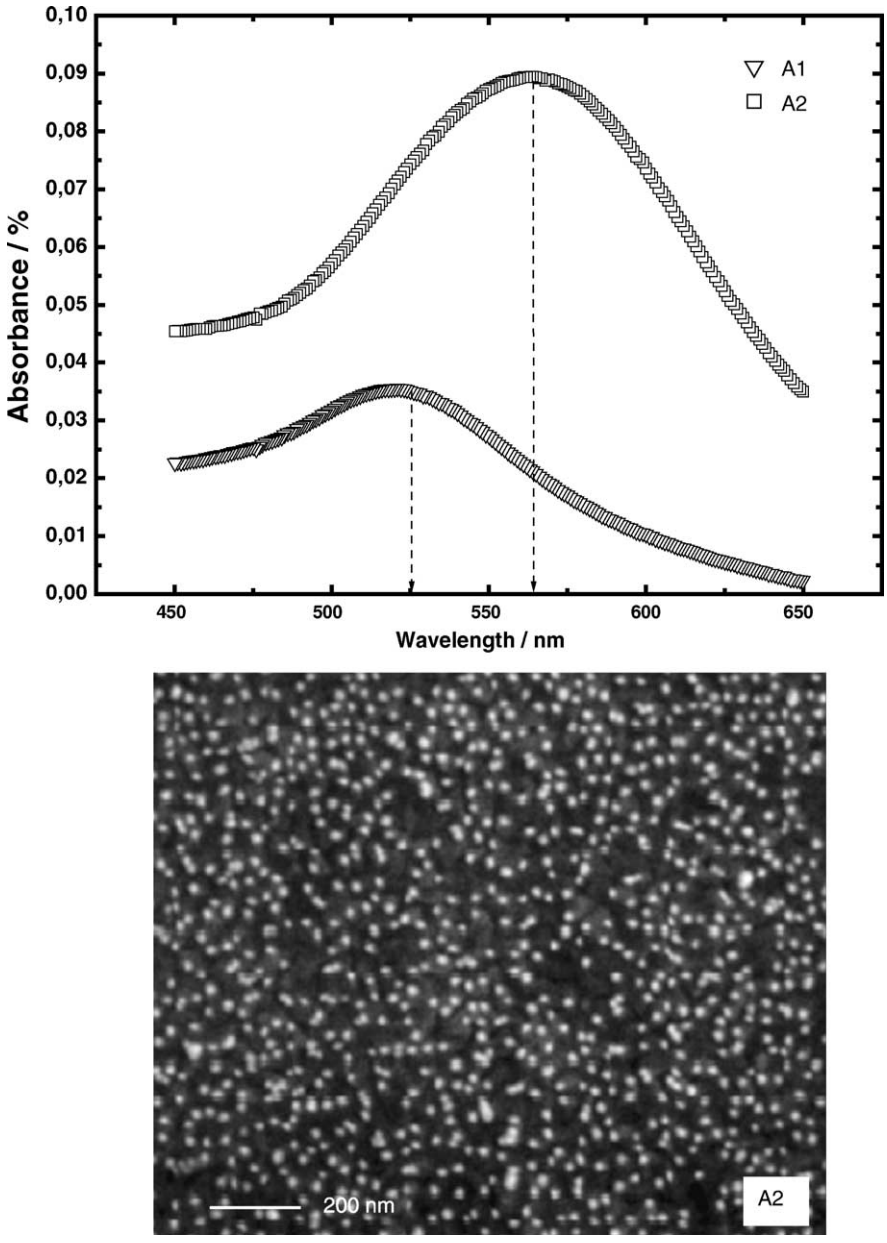

Fig. 2. SEM picture and UV–vis measurements in the 450–650 nm wavelength range for the clean AuNPs (A1 curve) and for the 1-dodecanethiol monolayer adsorbed on AuNPs (A2 curve), fixed on glass with the 3-(aminopropyl)trimethoxysilane intermediate. The dashed lines indicate the SPR maximum.

interface (sample A2) both show a well-defined surface plasmon resonance (SPR), much stronger for sample A2. The maximum is located at 525 and 565 nm, respectively, i.e. near the 532 nm wavelength of the incident visible beam in SFG configuration. The SPR maximum position for sample A1 is in accordance with similar works on gold colloidal solutions and clean AuNPs films [1,10]. We may note that molecular adsorption induces a redshift of the SPR maximum position.

For the samples with the 3-(mercaptopropyl) trimethoxysilane intermediate (Fig. 3), the SPR are measurable for both samples but these AuNPs films exhibit a strongly damped plasmon band compared to Fig. 2, which is attributed to a chemical interface damping. Indeed, the SEM picture of Fig. 3 shows two differences with Fig. 2: the density of AuNPs aggregates is more important whereas the mean coverage is lower. These observations prove that method 1 is better than method 2 with regard to the homogeneity of the AuNPs films, which is crucial to obtain large SAMs domains and efficient optical properties. In addition, we observe major differences between the UV–vis curves features of samples B1 and B2 for which we cannot even clearly locate a SPR maximum in the probed spectral range. They may be related to the nature of the molecules involved in the adsorption process. It is thus clear that the 2-aminoethanethiol molecules strongly affect the optical surface properties of the AuNPs film.

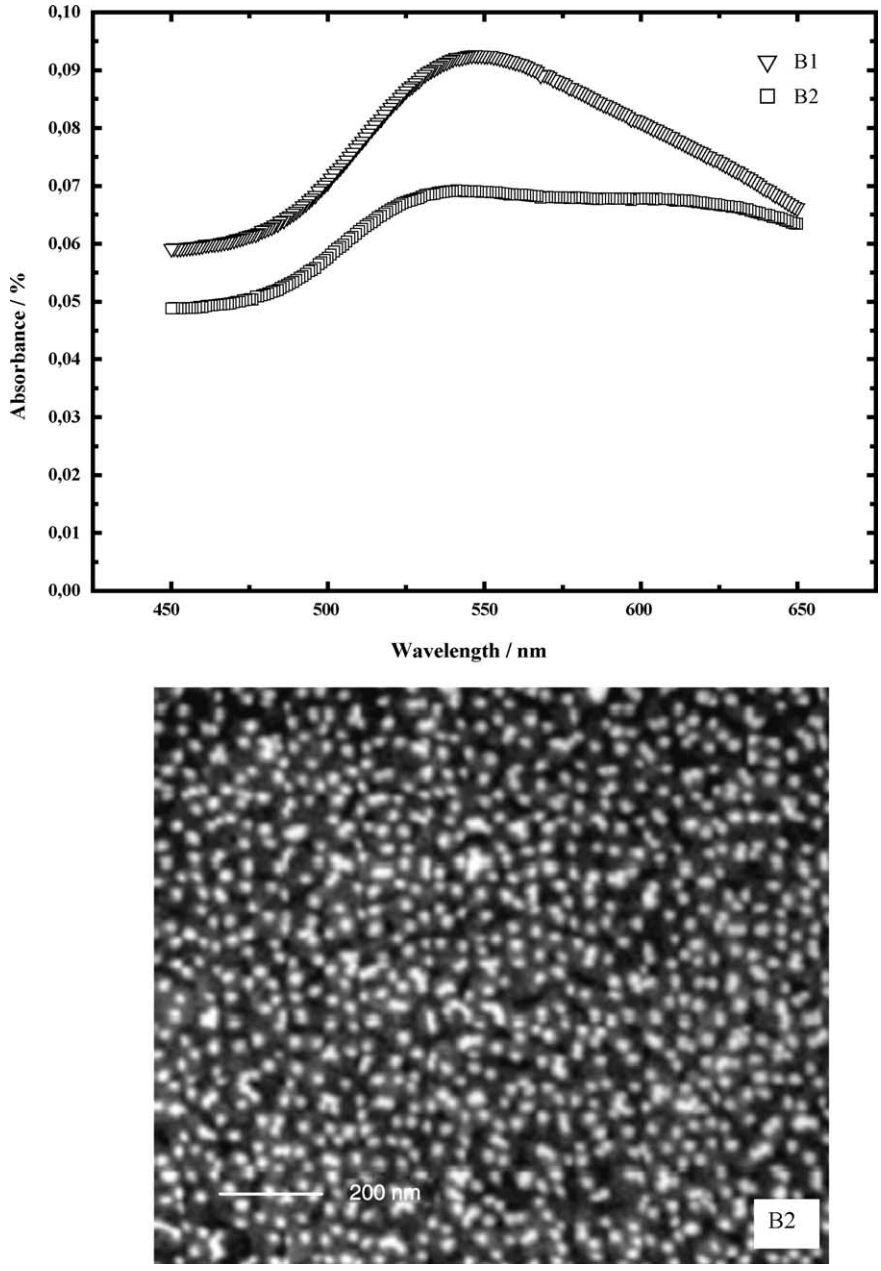

Fig. 3. SEM picture and UV–vis measurements in the 450–650 nm wavelength range for the 1-dodecanethiol monolayer adsorbed on AuNPs (B1 curve) and for the 2-aminoethanethiol monolayer adsorbed on AuNPs (B2 curve), fixed on glass with the 3-(mercaptopropyl)triethoxysilane intermediate.

Finally, the effect of the treatment applied to samples C appears in Fig. 4. In this case, we obtain again well-defined SPR, with their maxima located at different wavelengths, as a function of the adsorbate nature. However, we may already note that the stronger SPR maximum is located near 560 nm for the deposited 1-dodecanethiol molecules (sample C1), analogous to what we observed in Fig. 2 (sample A2). Samples A2 and C1 exhibit in fact very alike UV–vis curves, leading us to consider that they have similar optical properties. This is confirmed by their SEM pictures, which show analogous surface homogeneity and density of AuNPs aggregates. It must be pointed out that increasing the surface coverage, and thus lowering the distance between AuNPs induces a clear redshift of the surface plasmon band due to quadrupole effects (samples A2 and C1).

4.2. SFG/DFG measurements

The SFG measurements are performed in the 2800–3000 cm^{-1} infrared spectral range in order to detect the terminal CH stretching vibration modes of the molecules forming SAMs on gold nanoparticles. In our experiments, only two 1-dodecanethiol samples, A2 and C1,

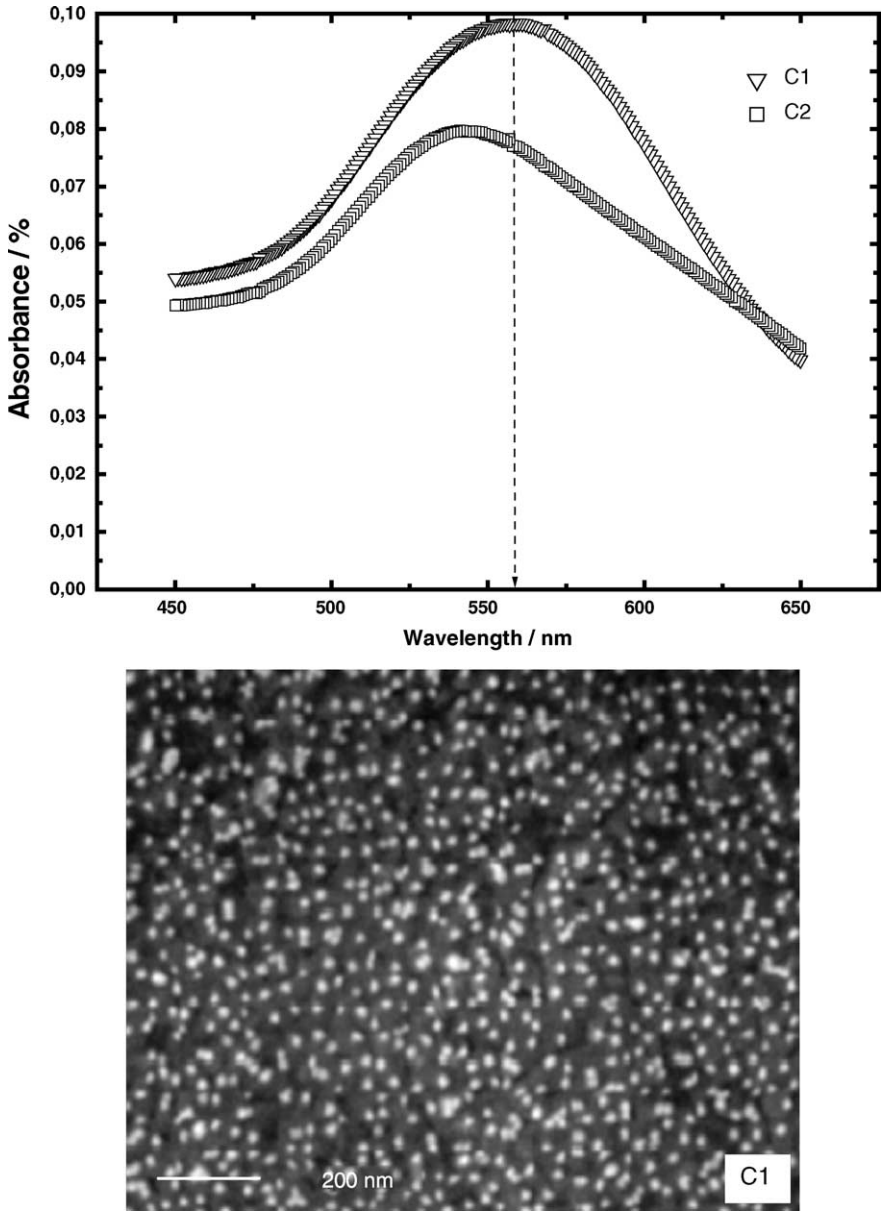

Fig. 4. SEM picture and UV–vis measurements in the 450–650 nm wavelength range for the 1-dodecanethiol monolayer adsorbed on AuNPs (C1 curve) and for the 2-aminoethanethiol monolayer adsorbed on AuNPs (C2 curve), fixed on glass substrate, after NaOH contact, with the 3-(mercaptopropyl)triethoxysilane intermediate. The dashed lines indicate the SPR maximum.

exhibit SFG vibrational features (Figs. 5 and 6). For all other samples, no SFG signal was detected.

On Fig. 5, we clearly see three vibration modes, interfering destructively with a rather constant SFG background coming from the AuNPs substrate. In keeping with previous SFG works on similar organic 1-dodecanethiol SAMs adsorbed on thick films or Au(1 1 1) single crystals [11], these vibration modes located at 2881, 2941 and 2968 cm^{-1} are related to the symmetric, Fermi resonance and degenerate stretching modes of the methyl CH_3 end-groups, respectively. Moreover, this spectrum exhibits two weaker vibration modes at ~2850 and ~2915 cm^{-1} related to the methylene CH_2 alkane chains symmetric and asymmetric stretching modes. The presence of these two latter modes and the ratio of the relative intensities of the CH_2 and CH_3 symmetric stretching modes are good indications of the order of the molecular chains within the SAMs. If this ratio is close to 0, it means that the alkane chains have few gauche defects and that the molecules are relatively well ordered within the organic film, with their CH_3 groups pointing out of the interface.

On Fig. 6, we also observe the CH_3 vibration modes but no obvious sign of the CH_2 stretching modes. This may originate from the weak signal-to-noise ratio, which is due to the fact that the SFG signals are very weak and not far above the detection threshold. However, at this stage, an increase of the incident laser beam energies intended to generate more

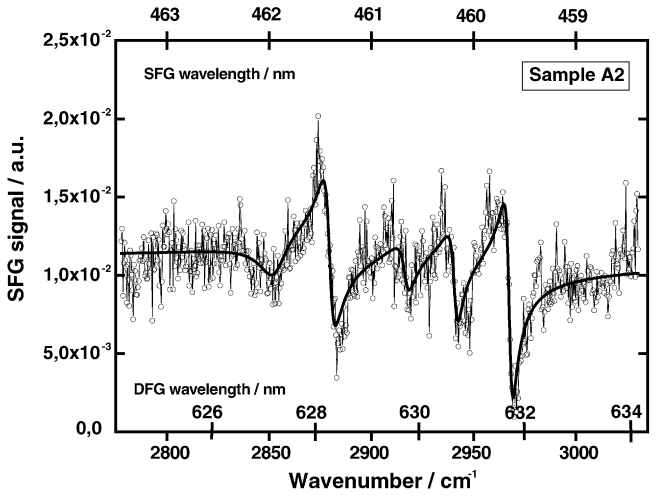

Fig. 5. SFG (ppp polarisation combination) spectrum of the A2 sample (see text for details). The theorethical fit is the black continuous line.

SFG would melt the films. Nevertheless, we consider that the differences in the CH_2 stretching mode region between the two spectra are significant and not only due to the quality of the data.

We equally tentatively performed SFG measurements on similar substrates with adsorbed 2-aminoethanethiol in the 2000–4000 cm^{-1} spectral range but it was unsuccessful: no SFG signal, neither resonant nor non-resonant, could be detected.

We could not detect any DFG signal of sample A2 and C1 contrary to what is expected on the basis of theoretical and experimental considerations made in previous combined SFG/DFG measurements on various metal interfaces in electrochemical conditions [12,13]. We only detect a weak fluorescence response decreasing with the energy. Considering the poor signal-to-noise ratio in Figs. 5 and 6, it is probable that the DFG photons are hidden by the intrinsic fluorescence inherent to this particular spectroscopy.

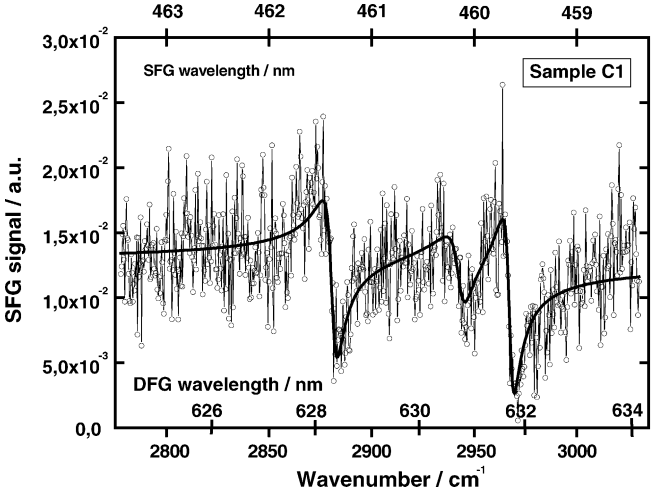

Fig. 6. SFG spectrum (ppp polarisation combination) of the C1 sample (see text for details). The theorethical fit is the black continuous line.

5. Discussion

In previous works [11,14], it was experimentally shown that the s–d interband electronic properties of Au(1 1 1) single crystals or thick Au(1 1 1) films was the physical process accounting for the interference patterns observed in SFG experiments and analogous to the spectra in Figs. 5 and 6. Using a visible laser source between 450 and 700 nm, the authors showed that the metal interband transition was resonant with the SFG frequency, but not the incident visible one. This idea was first suggested by Le Rille and co-workers, working in electrochemical conditions on gold electrodes [12,13]. In order to detect the weak non-linear response of adsorbed molecular species on gold substrate without being disturbed by the metal non-resonant contribution to the SFG signal, they performed DFG measurements. Indeed, as the interband s–d transition was located at ∼480 nm in their experimental conditions, i.e. in the probe SFG energy range, they chose to work in DFG detection, i.e. at ∼630 nm.

In our SFG measurements, it seems that an additional electronic process is involved in the generation of the interface SFG signal. Our visible incident beam at 532 nm is near the maximum of the SPR (560 nm) in both samples A2 and C1 where the adsorbate SFG response is detected. On the contrary, the SFG and DFG wavelengths are near 460 and 630 nm, respectively, i.e. far from the SPR resonance energy. This is why we make the hypothesis that these two generated beams cannot excite such a resonance and that only the incident visible beam is responsible for the SFG signal enhancement through SPR excitation. Indeed, a giant enhancement of optical second harmonic generation (SHG) signal is predicted for metal spheres [15] with respect to a plane surface. As SHG can be seen as a particular case of SFG theory, similar behaviours could be expected when lightening the samples with the 532 nm wavelength incident beam. At a molecular level, the absorption of light by the well-organized AuNPs results in a coherent collective oscillation of the conduction band free electrons induced by the visible electromagnetic field. This effect, predicted in the Mie theory [16] and predominant in the electronic properties of AuNPs, is better correlated to the SFG signal behaviour than the interband transition. This linear optical process generates a strong perpendicular surface electromagnetic local field. This one couples to the coherent non-linear optical SFG process through the normal components of the second order non-linear susceptibility tensor of the interface, and therefore amplifies the signal. In this way, the observation of the methyl vibration modes can be favourable if their dipolar moments are aligned with the enhanced normal components of the fields at the AuNPs surface [4].

In the case of 2-aminoethanethiol molecules interfaces, two reasons may explain the absence of SFG signal. The first one is that the 2-aminoethanethiol molecules do not form an ordered SAM on such substrates. The other one is that the electronic properties at the interface are modified by the nature of the adsorbate molecules in a manner that it is not

possible to induce a coherent non-linear optical SFG process. This second hypothesis seems to be correlated with the UV–vis measurements on Figs. 2–4 for each sample. Sum-frequency is thus generated only at interfaces showing a strong, well-defined SPR peak in the UV–vis spectra. The combination of SEM pictures and UV–vis spectra indicates that this is achieved when the overall density of AuNPs is high but that of aggregates low, and that the silanisation step is crucial for that respect. In addition, the molecule adsorbed on the AuNPs may have a positive (1-dodecanethiol) or negative influence (2-aminoethanethiol) on the linear optical properties, and thus strongly condition the spectroscopic analysis by SFG.

At this stage, it is interesting to note that an electrochemical control of the AuNPs electrode potential may induce variations in the electric field components at the interface and therefore modify its molecular adsorption properties and SFG activity. Combining in situ electrochemistry and SFG on AuNPs films in order to characterize them in a controlled interface conformation as it is commonly done on Au single crystals (electrodes) or films [12,13] is thus an attractive challenge.

In order to discuss the conformational information extracted from the SFG data, we summarize here the way we fit our SFG spectra in Figs. 5 and 6. SFG is a coherent process whose intensity is described by [17]:

$$I(\omega_{\mathrm{SFG}}) \propto |\chi_{\mathrm{NR}} + \chi_{\mathrm{R}}|^2 = \left| |\chi_{\mathrm{NR}}| e^{i\Phi} + \sum_{q=1}^{n} \left| \frac{|a_q| e^{i\varphi}}{\omega_q - \omega_{\mathrm{IR}} + i\Gamma_q} \right| \right|^2 \quad (1)$$

where χ_{NR} and χ_{R} are the second order non-linear susceptibilities of the AuNPs non-resonant signal and of the 1-dodecanethiol molecules resonant signal, respectively. n is the number of considered vibration modes. This expression contains complex amplitudes, including a phase shift $(\Phi - \varphi)$ between these two distinct contributions to the SFG intensity. This explains the interference pattern observed in the spectra in Fig. 5 ($n = 5$) and Fig. 6 ($n = 3$). a_q is the complex amplitude of the qth vibration mode with ω_q frequency and Γ_q damping constant, taking account of infrared and Raman selection rules as detailed in [14]. The vibration modes are supposed to have a homogeneous broadening, which explains the presence of Lorentzian oscillators in Eq. (1). The fit curves are drawn in Figs. 5 and 6, with the corresponding parameters displayed in Tables 1 and 2. We arbitrarily fixed each phase of the methyl (CH_3) vibration modes to 0 in order to simplify the fitting procedure. Indeed, the phase parameters (φ) could theoretically vary due to the various symmetries of these modes and to the interference between two close modes. An illustration is given in Fig. 5 and Table 1 for the symmetric stretching methyl and methylene modes. We chose to let φ vary for the CH_3 symmetric stretching mode to get a better correlation with the experimental data. However, this does hardly change the values deduced for the key parameters a, ω and Γ. In a general way, with a fixed visible wavelength at 532 nm, the electronic properties of the 1-dodecanethiol molecules are not modified in our probe energy range as illustrated in [14]. This explains why it is sufficient to keep $\varphi = 0$, making the hypothesis that the molecules are relatively well ordered and the vibration modes not interfering as observed in Fig. 6. In these conditions, we observe a strong correlation between the experimental SFG data and this simplified simulation procedure.

Eq. (1) shows why the interfacial SFG response exhibits a strong interference pattern between the non-linear activities of the AuNPs and the 1-dodecanethiol molecules, as illustrated in Tables 1 and 2 by the important phase shift ($\Phi - \varphi > 2.5$ rad). Even if the interband activity of the second order non-resonant susceptibility of AuNPs is not involved in the enhancement of the SFG signal at the interface due to its weak amplitude ($A \leq a_q$), this is the physical origin of the interference pattern [11,14].

We consider that the lower ratio between CH_2 and CH_3 symmetric stretching modes is an evidence of a better order in the alkane chains in sample C1 than in sample A2. This has been made possible thanks to method C, which improved wettability of the glass substrates. Basically, the surface sites of a native substrate are Si–H or Si–OH. Because of the strong pH modification induced by the aqueous solution of NaOH (3 M), the glass surface is made completely hydrophilic, i.e.

Table 1
Parameters set obtained from the fitting with Eq. (1) of the SFG signal in Fig. 5

Substrate					
Parameters					χ_{NR}
A					0.104601
Φ (rad)					2.54119
Adsorbate					
Parameters	CH_3–SS	CH_3–FR	CH_3–DS	CH_2–SS	CH_2–AS
ω_q (cm^{-1})	2879.57	2940.83	2967.54	2852.75	2916.84
Γ_q (cm^{-1})	3.04369	2.54476	2.17197	7.84061	3.27013
$\|\|a_q\|\|$	0.137187	0.0743117	0.162334	0.091664	0.0481327
φ_q (rad)	−0.345436	0	0	1.27836	0.0296674

Table 2
Parameters set obtained from the fitting with Eq. (1) of the SFG signal in Fig. 6

Substrate	
Parameters	χ_{NR}
A	0.112784
Φ (rad)	2.53363

Adsorbate			
Parameters	CH_3–SS	CH_3–FR	CH_3–DS
ω_q (cm^{-1})	2880.85	2942.86	2967.39
Γ_q (cm^{-1})	3.37492	4.58222	2.80217
$\|\|a_q\|\|$	0.19853	0.116988	0.214321
φ_q (rad)	0	0	0

the Si–OH surface sites are largely favoured. Consequently, Si–O–Si bounds created in the silanisation process are more numerous than in B samples. It implies therefore that there are more AuNPs fixed on the silanes, closer from each other; typically, they are 15 nm apart in such conditions instead of 25 nm prior to the treatment. This gives us a more compact surface but comprising less aggregates as observed by comparison of SEM pictures in Figs. 3 and 4. We thus have a better-ordered AuNPs set with more identical adsorption sites for the thiol molecules. In this case, it is interesting to note that the intrinsic sensitivity of SFG spectroscopy to the surface order gives information on the SAM adsorbate quality, directly related to the substrate preparation, by revealing the vibrational activity of the coherently oriented CH_3 end-groups.

6. Conclusion and perspectives

We showed that a non-linear optical vibrational spectroscopic tool such as sum-frequency generation may apply to self-assembled monolayers of 1-dodecanethiol adsorbed on gold nanoparticles films. The SFG sensitivity to the molecular vibration modes depends on the AuNPs ordering (density of AuNPs and density of aggregates) on the glass substrate and on the nature of the adsorbed molecules. This is directly related to the quality of the silanisation process. When the intermediate used to fix the AuNPs is correctly chosen, and additionally when the hydrophilicity of the glass is improved, surface plasmon resonance is well marked around 560 nm. In that case, the sum frequency generation is enhanced through a coupling of the incident visible pump (532 nm) at the interface to the surface plasmon, and a SFG signal can be detected. The features of the SFG spectra depend on the classical interference phenomenon between the s–d interband activity of the AuNPs substrate and the molecular properties of the adsorbate. Finally, we were able to estimate the order inside the molecular layer deposited on the AuNPs for the SFG-active samples.

In the near future, the use of a new emerging technique, two-colour sum-frequency generation spectroscopy (2C-SFG), which takes advantage of a tuneable visible wavelength, should give a more precise understanding of this complex phenomenon. Indeed, we will be able to continuously probe the SPR range and study the coupling processes between the AuNPs and the adsorbed species.

This kind of measurements show the ability of SFG/DFG/2C-SFG to be used as in situ spectroscopies of the structure and chemistry of AuNPs and adsorbed molecules. They appear as efficient candidates to overcome the weakness of the optical activity generated by such objects due to their very low amount of material. This should be enhanced in electrochemical conditions, thanks to the strong electric field on the working electrode. Furthermore, the characterisation of controlled AuNPs networks is of fundamental interest as precursors to the manufacturing of molecular and biological sensors, at the monolayer level development in real time, whereas the electrochemical processes occur.

Acknowledgements

C.H. is Scientific Research Worker of the Belgian National Fund for Scientific Research (F.N.R.S.) and thanks the Laboratoire pour l'Utilisation du Rayonnement Electromagnétique (LURE, CNRS-UMR 130), for having the possibility of doing this work.

References

[1] M.-C. Daniel, D. Astruc, Chem. Rev. 104 (2004) 293.
[2] R. Antoine, P.F. Brevet, H.H. Girault, D. Bethell, D.J. Schiffrin, Chem. Commun. 19 (1997) 1901.
[3] Y.C. Shen, Z.M. Tang, M.Z. Gui, J.Q. Cheng, X. Wang, Z.H. Lu, Chem. Lett. 10 (2000) 1140.
[4] T. Kawai, D.J. Nevandt, P.B. Davies, J. Am. Chem. Soc. 122 (2000) 12031.
[5] G.A. Somorjai, Appl. Surf. Sci. 121 (1997) 1.
[6] T. Dellwig, G. Rupprechter, H. Unterhalt, H.J. Freund, Phys. Rev. Lett. 85 (2000) 776.
[7] G. Rupprechter, H.J. Freund, Top. Catal. 14 (2001) 3.
[8] J. Turkevich, P.C. Stevenson, J. Hillier, J. Disc. Faraday Soc. 11 (1951) 55.

[9] A.A. Mani, L. Dreesen, P. Hollander, C. Humbert, Y. Caudano, P.A. Thiry, A. Peremans, Appl. Phys. Lett. 79 (2001) 1945.
[10] J.-P. Abid, Ph.D. Thesis and References Therein, 2003. Ecole Polytechnique Fédérale de Lausanne, Switzerland.
[11] L. Dreesen, C. Humbert, M. Celebi, J.-J. Lemaire, A.A. Mani, P.A. Thiry, A. Peremans, Appl. Phys. B 74 (2002) 621.
[12] A. Le Rille, A. Tadjeddine, W.-Q. Zheng, A. Peremans, Chem. Phys. Lett. 271 (1997) 95.
[13] A. Tadjeddine, O. Pluchery, A. Le Rille, C. Humbert, M. Buck, A. Peremans, W.Q. Zheng, J. Electroanal. Chem. 473 (1999) 25.
[14] C. Humbert, L. Dreesen, A.A. Mani, Y. Caudano, J.-J. Lemaire, P.A. Thiry, A. Peremans, Surf. Sci. 502-503 (2002) 203.
[15] D. Östling, P. Stampfli, K.H. Bennemann, Z. Phys. D 28 (1993) 169.
[16] G. Mie, Ann. Phys. 25 (1908) 377.
[17] A.V. Petukhov, Phys. Rev. B 52 (1995) 16901.